Journal of Photochemistry & Photobiology, B: Biology 153 (2015) 1–6

Contents lists available at ScienceDirect

Journal of Photochemistry & Photobiology, B: Biology

journal homepage: www.elsevier.com/locate/jpb

Physiological response of marine centric diatoms to ultraviolet radiation, with special reference to cell size

Yaping Wu [a,*], Zhenzhen Li [a], Wanjun Du [b], Kunshan Gao [a]

[a] State Key Laboratory of Marine Environmental Science, Xiamen University, Xiamen, China
[b] School of Environment and Natural Resources, Renmin University of China, Beijing, China

ARTICLE INFO

Article history:
Received 27 June 2015
Received in revised form 20 August 2015
Accepted 21 August 2015
Available online 8 September 2015

Keywords:
Cell size
Diatom
Photosystem
Thalassiosira
UV radiation

ABSTRACT

Three centric diatoms, *Thalassiosira pseudonana* (diameter ~4 μm), *Thalassiosira weissflogii* (~11 μm), and *Thalassiosira punctigera* (~47 μm), were exposed to low and high levels of UV radiation. UV-induced inhibition on photosystem II was correlated with cell size under high light levels, though it was insignificant under low light levels (PAR < 63 W m^{-2}). The highest inhibition (~15%) was observed for the smallest species. Several mechanisms may explain the observed relationship between cell size and response to UV. All three species counteracted UV-related photosystem damage via protein synthesis within the chloroplast. Non-photochemical quenching (NPQ) was induced when that process was blocked with an inhibitor in *T. pseudonana* and *T. weissflogii*, but not *T. punctigera*, as neither radiation nor the inhibitor had a significant effect on NPQ in this species. Moreover, UV-induced inhibition for cells treated with lincomycin was highest for *T. weissflogii*, which was in accordance with the highest UV exposure within the cell. The intracellular UV distribution was not associated with cell size, indicating that the package effect was not the only determinant of cell-size dependent UV sensitivity in phytoplankton.

1. Introduction

Phytoplankton in the euphotic zone utilize sunlight for photosynthesis, but may also be harmed by ultraviolet (UV) radiation at shallower depths [1]. The biological effects of UV radiation depend on wavelength [2]; the most detrimental radiation (UVC) is completely filtered out by diatomic oxygen and ozone, while the intensity of UVB is negatively correlated with the thickness of the ozone layer [3]. Though the use of CFC gases has been prohibited since the Montreal Protocol was established, some newly identified trace gases, such as halohydrocarbons, also destroy the ozone layer, resulting in increased UV radiation [4]. The precise effects of UV radiation in aquatic as well as terrestrial environments are still uncertain [5]. Phytoplankton that are exposed to high levels of UV radiation may be at risk for damage associated with climate change [6,7].

As the most productive phytoplankton group, diatoms account for 20% of the global primary production and play a fundamental role in the marine food web due to their abundance and size structure [8]. In particular, large diatoms contribute substantially to buried carbon owing to their high carbon content and fast sinking rate [9,10]. Therefore, the responses of differently sized diatoms to UV radiation may impact primary production and carbon export [9]. In theory, larger phytoplankton should be more resistant to UV radiation owing to package effects, i.e., more self-shading occurs in large than in small cells [11,12]. However, it is still unclear whether larger cells have more diluted pigments that would offset package effects, at least partially [13].

Field studies have been conducted to investigate the relationship between cell size and UV sensitivity, but the results of these studies vary. Some studies suggested that cell size is not a good indicator of UV sensitivity [14], but a recent study showed that photosynthetic carbon fixation of small phytoplankton was much more sensitive to UV than that of larger species in a coastal area [15]. At the molecular level, small cells are vulnerable to cyclobutane pyrimidine dimer accumulation, and photosynthesis is less inhibited by UV radiation [16], which may be attributed to faster photo-repair of small cells [17]. The light absorbed and scattered by cytoplasmic inclusion is an important determinant of the effects of UV on photosynthesis [11]. Additionally, phytoplankton species with differential pigments, geometry, and sub-cellular structures could differ significantly with respect to the intracellular light regime, and thus the UV exposure of photosynthetic organelles [11]. Figueroa et al. found that the bio-optical characteristics of a culture [18], rather than cell size or chlorophyll concentration, determine UV sensitivity. An intraspecific comparative analysis has shown that large species are less sensitive to UV than smaller species [19], indicated that the differences among species may outweigh the size effects; for example, *Phaeodactylum tricornutum* was more sensitive than *Thalassiosira pseudonana*, despite their similar sizes [20].

* Corresponding author.
E-mail address: yapingwu@xmu.edu.cn (Y. Wu).

http://dx.doi.org/10.1016/j.jphotobiol.2015.08.035
1011-1344/

The relationships between light absorption, cell size, and photosynthesis have been investigated [11,21,22], and recent studies have revealed a strong correlation between cell size and photo-inactivation in centric diatoms under high-PAR conditions [23]. Few laboratory studies have examined the UV responses of diatoms of various sizes, particularly using closely related species, which are expected to differ minimally with respect to traits such as cell geometry and pigmentation. In this study, we selected three species within the genus *Thalassiosira* that ranged in cell diameter from ~4 to ~47 μm to determine whether UV sensitivity is correlated with cell size and the underlying mechanisms that mediate this relationship.

2. Materials and Methods

2.1. Species and Culture Conditions

Thalassiosira weissflogii (CCMA102, ~11 μm) was isolated from the South China Sea in 2004 and obtained from the Center for Collection of Marine Bacteria and Phytoplankton (CCMA) of Xiamen University. *T. pseudonana* (CCMP1335, ~4 μm) was obtained from the National Center for Marine Algae and Microbiota (NCMA). *Thalassiosira punctigera* (CCAP 1085/19, ~47 μm) was obtained from the Culture Collection of Algae and Protozoa (CCAP).

Cells were inoculated in pre-aerated, sterilized filtered seawater and enriched with Aquil medium. Cultures were maintained semi-continuously with a maximal chlorophyll concentration of below 20 μg L^{-1} in polycarbonate bottles (500 mL). Cultures were illuminated with cool fluorescent tubes at a photon flux density of ~200 μmol m^{-2} s^{-1}, with a 12:12 light/dark cycle at 20 ± 1 °C, and culture bottles were manually shaken 3–4 times per day and then randomly distributed in the growth chamber.

2.2. Determination of Cell Absorbance, Chlorophyll Concentration, and Size

The 100-mL cultures (or media for blanks) were filtered on GF/F filters, and then gently attached to the filter holder in the spectrophotometer, which was equipped with an integrating sphere (Lambda950, PerkinElmer, Waltham, MA, USA). The absorbance was scanned between 280–750 nm and corrected using the blank filter. After measurements, filters were immediately extracted in absolute methanol for 2 h at room temperature and centrifuged. The supernatant was measured with a spectrophotometer (DU800, Beckman, Pasadena, CA, USA), and the chlorophyll concentration was calculated according to the methods of [24]. Cell size was measured under a microscope calibrated with a micrometer [25].

2.3. Experimental Set-up

The experiments were conducted under a solar simulator (Sol 1200, Hönle, Gräfelfing, Germany) with a 1000-W xenon arc lamp as a light source. Measurements of UV-B light (280–315 nm), UV-A (315–400 nm), and PAR (400–700 nm) were obtained using a broadband radiometer (PMA2100, Solar Light, USA). While the spectrum of UV within the quartz tube which covered with Ultraphan 295 filter, was measured with a spectrometer (HR4000, Ocean Optics, USA).

In the middle of the light period, cells in the exponential phase were harvested and transferred to quartz tubes (50 mL) directly at a density of less than 20 μg chl-a L^{-1}, dark-adapted for 15 min, and added with lincomycin (final concentration, 0.5 mg mL^{-1}) or milli-Q water (as a control). The tubes were then covered with Ultraphan 295 or 395 filters, which block radiation below 295 or 395 nm, respectively, to create PAR + UV-A + UV-B (PAB) and PAR treatments. Tubes were then incubated in a water bath under the solar simulator, and the temperature was controlled with a cooling system (CTP3000, Eyela, Tokyo, Japan). Two light levels were applied consecutively (for 60 min each) using a neutral-density mesh. The low-light conditions were PAR = 63.2 W m^{-2} and UVR = 13.1 W m^{-2}; high light conditions were PAR = 141.7 W m^{-2} and UVR = 35.1 W m^{-2}. Chlorophyll fluorescence was measured with an XE-PAM fluorometer (Walz, Eichenring, Germany) before and during light exposure at a time interval of 12 min.

2.4. Chlorophyll Fluorescence Measurements

A total of 12 tubes (four treatments) were dark-adapted for 15 min, and sub-samples were taken from each tube to measure the initial chlorophyll fluorescence with the XE-PAM. The quartz tubes containing the samples were placed in a water bath under low-light levels. After five rounds of measurements (60 min), samples were exposed to high-light levels by removing the neutral density screen, and measured following the same procedure.

2.5. Data Analysis

Photochemical yield and non-photochemical quenching (NPQ) were measured with the XE-PAM and calculated according to the following equations:

$$\text{Photochemical yield} = (F_m' - F_t)/F_m'$$

$$\text{NPQ} = (F_m - F_m')/F_m,$$

where F_m is the dark-adapted maximal fluorescence, F_m' is the effective maximal fluorescence, and F_t is the steady-state fluorescence under actinic light.

The relative inhibition of photochemical yield by UV was estimated according to the following equation:

$$\text{Relative inhibition}(\%) = (P_{PAR} - P_{PAB})/P_{PAR} \times 100,$$

where P_{PAR} and P_{PAB} represent the photochemical yield under PAR and PAB treatments, respectively. Relative inhibition was calculated when P_{PAR} and P_{PAB} were significantly different. Statistical differences among treatments were analyzed with a one-way analysis of variance (ANOVA) and Tukey's test, and the significance level was set at $p = 0.05$.

To estimate the UV distribution within the cell, cells were assumed to be spherical with an even distribution of pigments. Several parameters, i.e., the spectral absorbance of filters with intact cells, spectrum of UV within quartz tube, and cell density on the membrane, were used to derive the attenuation coefficient of UV radiation (280–400 nm). The relative UV intensity was plotted as a function of the optical length from the cell surface. The attenuation coefficient for UV was calculated as:

$$k_{uv} = -\text{Ln}\frac{\int_{\lambda=280}^{400nm} E_\lambda * T_\lambda}{\int_{\lambda=280}^{400nm} E_\lambda} \div L,$$

where E_λ is the relative UV intensity within the quartz tube, T_λ is the transmittance (in percentage) of the algal mat on the filter, while L (μm) represents the thickness of the algal mat.

The rate of UVR-induced damage to photosystem II (PSII) (k, min^{-1}) and the corresponding repair rate (r, min^{-1}) were calculated according to the following equation of [26]:

$$\frac{P_0}{P_t} = \frac{r}{k+r} + \frac{k}{k+r}e^{-(k+r)t},$$

where P_0 and P_t represent the initial photochemical yield or at a certain time point, respectively, and t is the exposure time in minutes.

3. Results

The dark-adapted photochemical yield was ~0.6 for *T. pseudonana*, and decreased immediately after exposure to low light. It remained relatively stable for control samples (without lincomycin) after incubation under low light, and no significant UV inhibition was observed for this light level (Fig. 1A). For the samples treated with lincomycin, the photochemical yield decreased gradually after low-light exposure, and was significantly lower for UV-exposed samples than control samples. When samples were exposed to high light, the photochemical yield of samples for all treatments decreased gradually toward the end of the incubation period, with lower values observed for UV-exposed samples (Fig. 1A). The trend observed for *T. weissflogii* was similar to that of *T. pseudonana*, while with higher dark adapted photochemical yields (~0.7) observed, the yields of lincomycin-treated samples decreased significantly, especially for UV-exposed samples (Fig. 1B). *T. punctigera* had the lowest dark-adapted photochemical yield, but the patterns observed under low and high light were similar to those of the other species (Fig. 1C), but with less reduction for lincomycin-treated samples during exposure to PAR or PAB. In addition, UV did not show significant effects on non-lincomycin-treated samples, even under high light conditions (Fig. 1C).

The relative UV-mediated inhibition of photochemical yield for control samples was almost zero for the three species under low light, with two outliers for *T. pseudonana* and *T. punctigera* (Fig. 2A). Under high light, UV inhibition was observed for *T. pseudonana* and *T. weissflogii*. UV inhibition was highest for the smallest species, and was not observed for the largest species, *T. punctigera* (Fig. 2A). For the lincomycin-treated samples, UV showed a significant inhibitory effect for all species. This effect increased as the low-light exposure time increased, while decreased over time under high light. *T. pseudonana* and *T. punctigera* showed similar responses to UV, while *T. weissflogii* exhibited higher UV sensitivity than that of the other species when treated with lincomycin (Fig. 2B). The relative UV-mediated inhibition at the end of the incubation period was negatively correlated with cell size, with highest value was observed for *T. pseudonana* (~15%), while lowest was observed for *T. punctigera* (0%) (Fig. 2C).

An important photo-protective mechanism, NPQ, ranged from 0–0.2 for the three species under low light without lincomycin, and there were no significant differences in NPQ between samples treated with PAR and PAB (Fig. 3). NPQ increased gradually for *T. pseudonana* and *T. weissflogii* samples treated with lincomycin (Fig. 3A, B), and was high for PAB-treated samples. After exposure to high light, the NPQ of *T. pseudonana* and *T. weissflogii* without lincomycin increased immediately under UV exposure. That of *T. pseudonana* samples treated with lincomycin decreased sharply, while *T. weissflogii* increased somewhat and was maintained at around 3.0 after high-light exposure (Fig. 3A,

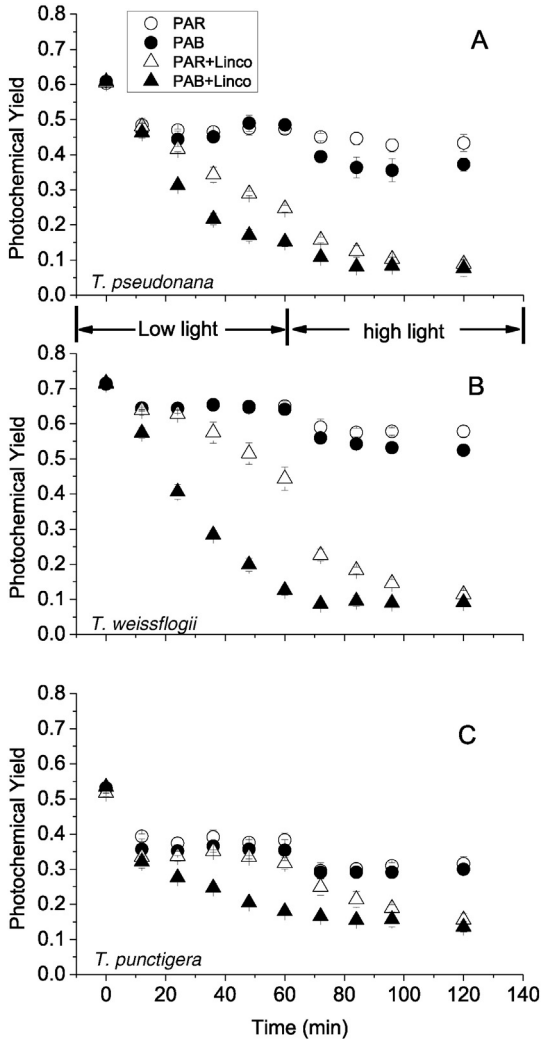

Fig. 1. The photochemical yield of *Thalassiosira pseudonana* (A), *T. weissflogii* (B), and *T. punctigera* (C) during exposure to low light (0–60 min) and the subsequent high light (61–120 min) for two radiation treatments (PAR and PAB) with or without lincomycin. Vertical lines represent standard deviations, n = 3.

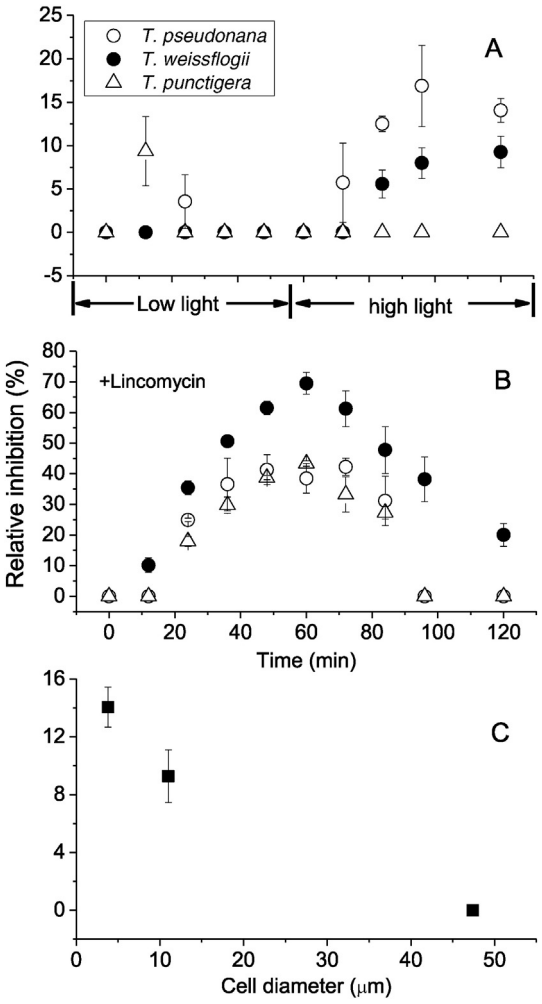

Fig. 2. The relative inhibition induced by UV radiation for three diatom species without (A) or with lincomycin (B) during low or high UV exposure, and the relative inhibition at the end of the incubation period for the control samples of the three species (C). Vertical lines represent standard deviations, n = 3.

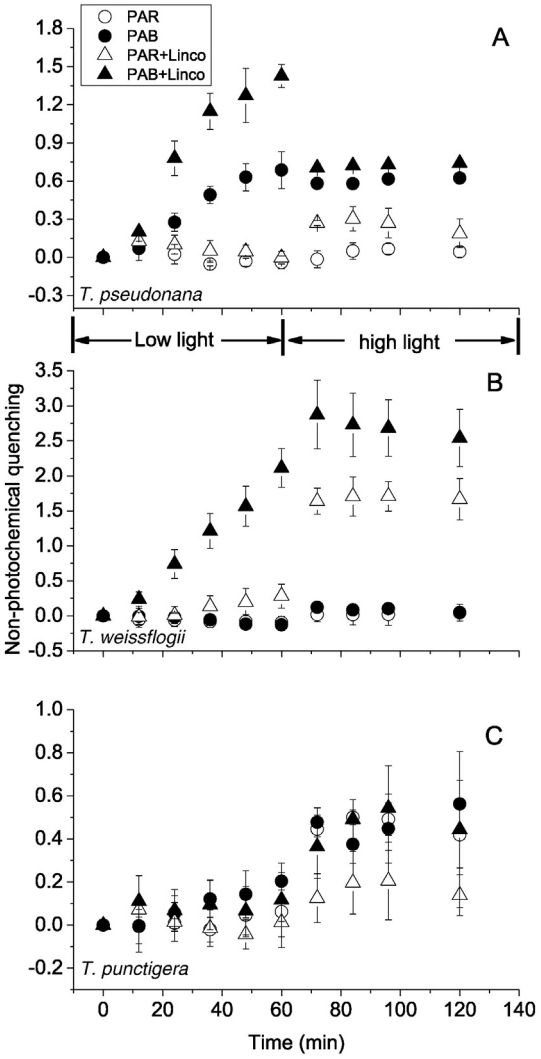

Fig. 3. Non-photochemical quenching of *T. pseudonana* (A), *T. weissflogii* (B), and *T. punctigera* (C) during exposure to low light (0–60 min) and the subsequent high light (61–120 min) for two radiation treatments (PAR and PAB) with or without lincomycin. Vertical lines represent standard deviations, n = 3.

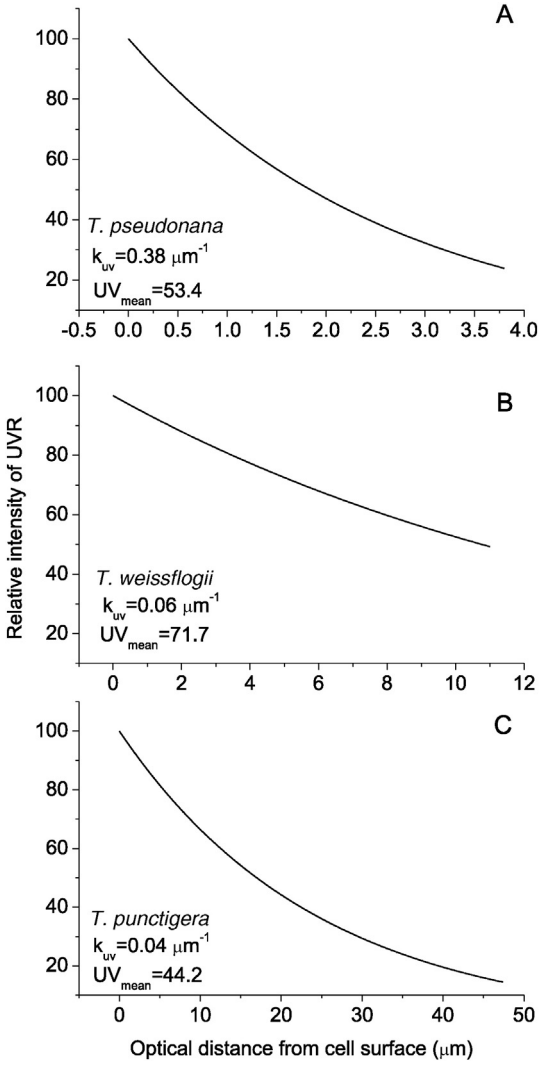

Fig. 4. The relative UV intensity within *T. pseudonana* (A), *T. weissflogii* (B), and *T. punctigera* (C) cells as a function of optical distance from the cell surface and the corresponding attenuation coefficients (μm^{-1}) for the UV waveband (280–400 nm) of solar simulator.

B). For *T. punctigera*, NPQ was approximately 0–0.2 under low light, but increased to ~0.5 under high light, and no significant differences were observed between samples treated with radiation or lincomycin (Fig. 3C).

The relative intensity of UV radiation was set at 100 at the cell surface, and the distribution of UV within cells exhibited exponential decay (Fig. 4), with attenuation coefficients of 0.37, 0.06, and 0.04 μm^{-1} for *T. pseudonana*, *T. weissflogii*, and *T. punctigera*, respectively. The distributions of UV for *T. pseudonana* and *T. punctigera* were similar (Fig. 4A, C), while relatively higher UV exposure within cells was observed for *T. weissflogii* (Fig. 4B). Specifically, the mean relative UV intensities were 53.4, 71.7, and 44.2 for *T. pseudonana*, *T. weissflogii*, and *T. punctigera*, respectively.

The absorption spectra of methanol extracts were similar for three species in the range of long wavelength (Fig. 5), while in the range of short wavelength of PAR and UV, the biggest diatom, *T. punctigera* showed relatively higher value, and *T. weissflogii* was the lowest.

The repair rates for non-lincomycin-treated samples were higher than the damage rates during light exposure (Table 1), even under UV exposure. For those samples treated with lincomycin, the repair rate of *T. weissflogii* was completely inhibited, while *T. pseudonana* and *T. punctigera* were able to partially repair photo-damage, though the repair rates were significantly lower than those of control samples.

4. Discussion

PSII converts light energy to electrons that drive carbon fixation in the Calvin cycle, but is susceptible to light, especially to high levels of

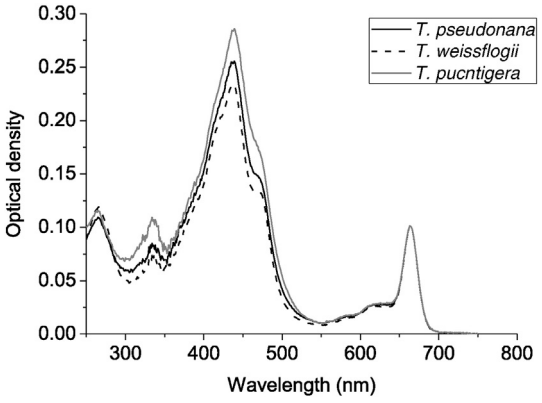

Fig. 5. Optical density of methanol extracts of three diatom species, values were normalized with OD set as 0.10 at 665 nm.

Table 1
Exponential rate constants (in min^{-1}) for repair (r) and damage (k) and the ratio of r to k for various radiation treatments with or without lincomycin (linco) for three centric diatom species.

Species	Treatment	r	SD	k	SD	r/k
Thalassiosira pseudonana	PAR + linco	0.0039	0.0019	0.0174	0.0009	0.2239
	PAB + linco	0.0023	0.0027	0.0283	0.0022	0.0814
	PAR	0.0556	0.0062	0.0172	0.0006	3.1998
	PAB	0.0889	0.0107	0.0280	0.0025	3.1727
T. weissflogii	PAR + linco	0	0	0.0072	0.0005	0
	PAB + linco	0	0	0.0247	0.0011	0
	PAR	0.0651	0.0097	0.0070	0.0004	9.0894
	PAB	0.2317	0.0084	0.0244	0.0010	9.3936
T. punctigera	PAR + linco	0.1053	0.0065	0.0433	0.0065	2.4328
	PAB + linco	0.0247	0.0067	0.0595	0.0160	0.4142
	PAR	0.1526	0.0438	0.0430	0.0062	3.5263
	PAB	0.0844	0.0061	0.0591	0.0166	1.4186

PAR or UV radiation [27]. Therefore, the susceptibility of PSII to UV radiation is a key determinant of marine primary production [28,29]. In the present study, UV-mediated inhibition of photochemical yield was apparently related to cell size, and the species with the smallest cells exhibited the highest sensitivities. This trend could not be explained by any single previously proposed theory, e.g., UV distribution within the cell, the dynamic balance between damage and repair processes, or NPQ, indicating that multiple mechanisms are involved in the size-dependent responses to UV radiation.

The three species used in present study have been cultured indoors for many years, and pre-acclimation before the experiments was under ~200 μmol m^{-2} s^{-1} (~40 W m^{-2}) without UV. Exposure to a comparable level of PAR or PAB (PAR 63.2 W m^{-2}, UVR 13.1 W m^{-2}) did not affect the photochemical yield, even under high light (PAR 141.7 W m^{-2}, UVR 35.1 W m^{-2}). The highest inhibition induced by UV was much lower than that of other species with comparable sizes [30,31], indicating that the damage repair capacity is highly efficient in this genus. For samples treated with lincomycin, dramatic UV-mediated inhibition was observed, and this inhibitory effect increased over time under low-light exposure, indicating that protein-dependent repair is one of the most important mechanisms mediating responses to UV [32].

UV radiation did not have significant effects on photochemical yield during low-light exposure. However, there was a species-specific effect under high light, and it was strongly related to cell size. After moving to high light, the smallest species, *T. pseudonana*, showed increased sensitivity to UV toward the end of the exposure, similar response observed for the medium size species, *T. weissflogii*, though with lower sensitivity than *T. pseudonana*. The largest species, *T. punctigera*, did not show any sensitivity to UV radiation, even under high light. On the whole, UV sensitivity was negatively correlated with cell size, and based on the intracellular UV distribution, this correlation could not be explained by the package effect, which has been proposed as a key determinant of UV sensitivity [12]. Indeed, the intracellular UV micro-environment influenced the effects of UV. Specifically, the medium-sized species, *T. weissflogii*, with highest mean intracellular UV intensity, showed the highest UV sensitivity when treated with lincomycin, suggesting that the in vivo absorbance of UV radiation is a determinant of UV sensitivity, that was also in accordance with the absorption of methanol extracts, *T. weissflogii* showed the lowest absorption in the range of UV, since UV-absorbing compounds synthesized by some species can greatly reduce UV-related damage [33].

D1 protein is the primary target in PSII for UV photo-damage, and is generated by *de novo* synthesis [34]. The balance between photodamage and repair is a key determinant of the maintenance of photosynthesis [35,36]. Although the pre-acclimation conditions were UV-free, the damage rate was always lower than the repair rate during low UV exposure, consistent with the low level of UV inhibition observed during this period. During subsequent high UV exposure, the damage rate was higher than the repair rate for *T. pseudonana* and *T. weissflogii*, which exhibited significant photosystem inhibition. Though the D1 renewal process was completely blocked by lincomycin, PSII repair in *T. pseudonana* and *T. punctigera* still occurred. However, repair was not observed for *T. weissflogii*, which may explain why it was the most sensitive species during UV exposure when treated with lincomycin.

NPQ is considered one of the most effective mechanisms for photoprotection [37]. During the transition from dark to light conditions, NPQ is normally induced; it is positively related to light intensity and affected by radiation spectra [38]. The NPQ values were around 0 for *T. pseudonana* and *T. weissflogii* under low light, and increased significantly when cells were treated with lincomycin, indicating that protein synthesis is the prior mechanism to counteract UV inhibition [30], while once that process was inhibited, NPQ played a key role in the response to UV stress. Interestingly, for *T. punctigera*, NPQ was less responsive to high-light exposure or the protein synthesis inhibitor, indicating that other mechanisms were adopted by this species to counteract UV damage.

The results of the present study showed that species in the genus *Thalassiosira* are more resistant to UV radiation than other species [30,31], and this could explain the wide distribution of this taxonomic group. Though UV sensitivity was related to cell size for the three species investigated, the mechanisms underlying this relationship are still uncertain. We suggested that cell size influences UV sensitivity, but that the responses of diatoms to UV cannot be predicted simply by cell size; instead, multiple factors have to be considered.

Acknowledgment

This study was supported by National Natural Science Foundation (41206091, 41430967, and 41120164007), the Fundamental Research Funds for the Central Universities (20720150076), Joint project of NSFC and Shandong province (Grant No. U1406403), and MELRI1403.

References

[1] D.-P. Häder, E.W. Helbling, C.E. Williamson, R.C. Worrest, Effects of UV radiation on aquatic ecosystems and interactions with climate change, Photochem. Photobiol. Sci. 10 (2011) 242, http://dx.doi.org/10.1039/c0pp90036b.
[2] J.J. Cullen, P.J. Neale, M.P. Lesser, Biological weighting function for the inhibition of phytoplankton photosynthesis by ultraviolet radiation, Science 258 (1992) 646–650, http://dx.doi.org/10.1126/science.258.5082.646.
[3] J. Staehelin, N.R.P. Harris, C. Appenzeller, J. Eberhard, Ozone trends: a review, Rev. Geophys. 39 (2001) 231–290, http://dx.doi.org/10.1029/1999RG000059.
[4] K.S. Law, W.T. Sturges, D.R. Blake, N.J. Blake, J.B. Burkholder, J.H. Butler, et al., Halogenated very short-lived substances, chapter 2, Scientific Assessment of Ozone Depletion: 2006, Global Ozone Research and Monitoring Project—Report No. 50World Meteorol. Organ., Geneva Switz. 2007, p. 572.
[5] R.R. Garcia, Atmospheric science: an Arctic ozone hole? Nature 478 (2011) 462–463, http://dx.doi.org/10.1038/478462a.
[6] J. Beardall, C. Sobrino, S. Stojkovic, Interactions between the impacts of ultraviolet radiation, elevated CO_2, and nutrient limitation on marine primary producers, Photochem. Photobiol. Sci. 8 (2009) 1257–1265, http://dx.doi.org/10.1039/B9PP00034H.

[7] G.L. Manney, M.L. Santee, M. Rex, N.J. Livesey, M.C. Pitts, P. Veefkind, et al., Unprecedented Arctic ozone loss in 2011, Nature 478 (2011) 469–475, http://dx.doi.org/10.1038/nature10556.
[8] E. Granum, J.A. Raven, R.C. Leegood, How do marine diatoms fix 10 billion tonnes of inorganic carbon per year? Can. J. Bot. 83 (2005) 898–908, http://dx.doi.org/10.1139/b05-077.
[9] Z.V. Finkel, J. Beardall, K.J. Flynn, A. Quigg, T.A.V. Rees, J.A. Raven, Phytoplankton in a changing world: cell size and elemental stoichiometry, J. Plankton Res. 32 (2010) 119–137, http://dx.doi.org/10.1093/plankt/fbp098.
[10] T. Kiørboe, Turbulence, phytoplankton cell size, and the structure of pelagic food webs, in: J. H. S. B., A.J. Southward (Eds.), Advances in Marine BiologyAcademic Press 1993, pp. 1–72.
[11] S. Agustí, Allometric scaling of light absorption and scattering by phytoplankton cells, Can. J. Fish. Aquat. Sci. 48 (1991) 763–767, http://dx.doi.org/10.1139/f91-091.
[12] T. Berner, Z. Dubinsky, K. Wyman, P.G. Falkowski, Photoadaptation and the "package" effect in *Dunaliella Tertiolecta* (Chlorophyceae), J. Phycol. 25 (1989) 70–78, http://dx.doi.org/10.1111/j.0022-3646.1989.00070.x.
[13] R.R. Bidigare, M.E. Ondrusek, J.H. Morrow, D.A. Kiefer, In-vivo absorption properties of algal pigments, 1990, pp. 290–302.
[14] I. Laurion, W.F. Vincent, Cell size versus taxonomic composition as determinants of UV-sensitivity in natural phytoplankton communities, Limnol. Oceanogr. 43 (1998) 1774–1779, http://dx.doi.org/10.4319/lo.1998.43.8.1774.
[15] G. Li, K. Gao, Cell size-dependent effects of solar UV radiation on primary production in coastal waters of the South China Sea, Estuar. Coasts 36 (2013) 728–736, http://dx.doi.org/10.1007/s12237-013-9591-6.
[16] E.W. Helbling, A.G.J. Buma, M.K. de Boer, V.E. Villafane, In situ impact of solar ultraviolet radiation on photosynthesis and DNA in temperate marine phytoplankton, Mar. Ecol. Prog. Ser. 43–49 (2001).
[17] A.G. Buma, P. Boelen, W.H. Jeffrey, UVR-induced DNA damage in aquatic organisms, UV Effects in Aquatic Organisms and Ecosystems, Royal Society of Chemistry, Great Britain 2003, pp. 291–327.
[18] F.L. Figueroa, J. Mercado, C. Jiménez, S. Salles, J. Aguilera, M.P. Sánchez-Saavedra, et al., Relationship between bio-optical characteristics and photoinhibition of phytoplankton, Aquat. Bot. 59 (1997) 237–251, http://dx.doi.org/10.1016/S0304-3770(97)00065-X.
[19] S.R. Halac, V.E. Villafañe, R.J. Gonçalves, E.W. Helbling, Photochemical responses of three marine phytoplankton species exposed to ultraviolet radiation and increased temperature: role of photoprotective mechanisms, J. Photochem. Photobiol. B 141 (2014) 217–227, http://dx.doi.org/10.1016/j.jphotobiol.2014.09.022.
[20] Y. Li, Physiological Responses and Mechanisms of Diatoms to Ocean AcidificationThesis Xiamen University, 2014.
[21] Z.V. Finkel, Light absorption and size scaling of light-limited metabolism in marine diatoms, Limnol. Oceanogr. 46 (2001) 86–94, http://dx.doi.org/10.4319/lo.2001.46.1.0086.
[22] Z.V. Finkel, A.J. Irwin, Light absorption by phytoplankton and the filter amplification correction: cell size and species effects, J. Exp. Mar. Biol. Ecol. 259 (2001) 51–61.
[23] T. Key, A. McCarthy, D.A. Campbell, C. Six, S. Roy, Z.V. Finkel, Cell size trade-offs govern light exploitation strategies in marine phytoplankton, Environ. Microbiol. 12 (2010) 95–104, http://dx.doi.org/10.1111/j.1462-2920.2009.02046.x.
[24] R.J. Ritchie, Consistent sets of spectrophotometric chlorophyll equations for acetone, methanol and ethanol solvents, Photosynth. Res. 89 (2006) 27–41, http://dx.doi.org/10.1007/s11120-006-9065-9.
[25] Y. Wu, D.A. Campbell, A.J. Irwin, D.J. Suggett, Z.V. Finkel, Ocean acidification enhances the growth rate of larger diatoms, Limnol. Oceanogr. 59 (2014) 1027–1034.
[26] P. Heraud, J. Beardall, Changes in chlorophyll fluorescence during exposure of *Dunaliella tertiolecta* to UV radiation indicate a dynamic interaction between damage and repair processes, Photosynth. Res. 63 (2000) 123–134, http://dx.doi.org/10.1023/A:1006319802047.
[27] D.A. Campbell, E. Tyystjärvi, Parameterization of photosystem II photoinactivation and repair, Biochim. Biophys. Acta 1817 (2012) 258–265, http://dx.doi.org/10.1016/j.bbabio.2011.04.010.
[28] S. Kataria, A. Jajoo, K.N. Guruprasad, Impact of increasing ultraviolet-B (UV-B) radiation on photosynthetic processes, J. Photochem. Photobiol. B Biol. 137 (2014) 55–66, http://dx.doi.org/10.1016/j.jphotobiol.2014.02.004.
[29] S. Long, S. Humphries, P. Falkowski, Photoinhibition of photosynthesis in nature, Annu. Rev. Plant Physiol. Plant Mol. Biol. 45 (1994) 633–662, http://dx.doi.org/10.1146/annurev.pp.45.060194.003221.
[30] Y. Wu, D.A. Campbell, K. Gao, Faster recovery of a diatom from UV damage under ocean acidification, J. Photochem. Photobiol. B 140 (2014) 249–254, http://dx.doi.org/10.1016/j.jphotobiol.2014.08.006.
[31] W. Guan, K. Gao, Light histories influence the impacts of solar ultraviolet radiation on photosynthesis and growth in a marine diatom, *Skeletonema costatum*, J. Photochem. Photobiol. B 91 (2008) 151–156, http://dx.doi.org/10.1016/j.jphotobiol.2008.03.004.
[32] S. Takahashi, M.R. Badger, Photoprotection in plants: a new light on photosystem II damage, Trends Plant Sci. 16 (2011) 53–60, http://dx.doi.org/10.1016/j.tplants.2010.10.001.
[33] P. Vale, Effects of light quality and nutrient availability on accumulation of mycosporine-like amino acids in *Gymnodinium catenatum* (Dinophycea), J. Photochem. Photobiol. B Biol. 143 (2015) 20–29, http://dx.doi.org/10.1016/j.jphotobiol.2014.12.016.
[34] S. Takahashi, N. Murata, Glycerate-3-phosphate, produced by CO_2 fixation in the Calvin cycle, is critical for the synthesis of the D1 protein of photosystem II, Biochim. Biophys. Acta 1757 (2006) 198–205, http://dx.doi.org/10.1016/j.bbabio.2006.02.002.
[35] A. Melis, Photosystem-II damage and repair cycle in chloroplasts: what modulates the rate of photodamage in vivo? Trends Plant Sci. 4 (1999) 130–135, http://dx.doi.org/10.1016/S1360-1385(99)01387-4.
[36] J. Grzymski, C. Orrico, O.M. Schofield, Monochromatic ultraviolet light induced damage to photosystem II efficiency and carbon fixation in the marine diatom *Thalassiosira pseudonana*, Photosynth. Res. 68 (2001) 181–192, http://dx.doi.org/10.1023/A:1012904402368.
[37] P. Müller, X.-P. Li, K.K. Niyogi, Non-photochemical quenching. A response to excess light energy, Plant Physiol. 125 (2001) 1558–1566, http://dx.doi.org/10.1104/pp.125.4.1558.
[38] N.R. Baker, Chlorophyll fluorescence: a probe of photosynthesis in vivo, Annu. Rev. Plant Biol., Annual Reviews, Palo Alto 2008, pp. 89–113.